ACS NANO

www.acsnano.org

ARTICLE

Single-Cell and Single-Molecule Analysis Unravels the Multifunctionality of the *Staphylococcus aureus* Collagen-Binding Protein Cna

Claire Valotteau,[†,∇] Valeria Prystopiuk,[†,∇] Giampiero Pietrocola,[‡,∇] Simonetta Rindi,[‡] Daniele Peterle,[§] Vincenzo De Filippis,[§] Timothy J. Foster,[∥] Pietro Speziale,*[,‡] and Yves F. Dufrêne*[,†,⊥]

[†]Institute of Life Sciences, Université Catholique de Louvain, Croix du Sud, 4-5, bte L7.07.06, Louvain-la-Neuve B-1348, Belgium

[‡]Department of Molecular Medicine, Unit of Biochemistry, University of Pavia, Viale Taramelli 3/b, Pavia 27100, Italy

[§]Laboratory of Protein Chemistry, Department of Pharmaceutical and Pharmacological Sciences, University of Padua, via F. Marzolo 5, Padova 35131, Italy

[∥]Department of Microbiology, Trinity College Dublin, Dublin 2, Ireland

[⊥]Walloon Excellence in Life sciences and Biotechnology (WELBIO), Liège 4000, Belgium

ABSTRACT: **The collagen-binding protein Cna is a prototype cell surface protein from *Staphylococcus aureus* which fulfils important physiological functions during pathogenesis. While it is established that Cna binds to collagen (Cn) *via* the high-affinity collagen hug mechanism, whether this protein is engaged in other ligand-binding mechanisms is poorly understood. Here, we use atomic force microscopy to demonstrate that Cna mediates attachment to two structurally and functionally different host proteins, *i.e.*, the complement system protein C1q and the extracellular matrix protein laminin (Lam), through binding mechanisms that differ from the collagen hug. We show that single Cna−C1q and Cna−Lam bonds are much weaker than the high-affinity Cna−Cn bond and that their formation does not require the B-region of Cna. At the whole cell level, we find that bacterial adhesion to C1q-substrates involves only one (or two) molecular bond(s), while adhesion to Lam is mediated by multiple bonds, thus suggesting that multivalent or cooperative interactions may enhance the strength of adhesion. Both C1q and Lam interactions can be efficiently blocked by monoclonal antibodies directed against the minimal Cn-binding domain of Cna. These results show that Cna is a multifunctional protein capable of binding to multiple host ligands through mechanisms that differ from the classical collagen hug.**

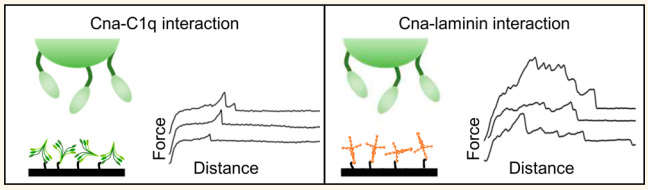

KEYWORDS: *atomic force microscopy, force spectroscopy, Staphylococcus aureus, Cna, C1q, laminin, binding mechanisms*

In the host extracellular matrix (ECM), a milieu composed of proteoglycans and fibrous proteins with both adhesive and structural functions such as collagen (Cn), elastin, fibronectin, and laminin (Lam), *Staphylococcus aureus* can bind a variety of proteins that are present. The ability to bind ECM proteins is a function of ligand-specific adhesins collectively referred to as microbial surface components recognizing adhesive matrix molecules (MSCRAMMs). Cna is a prototype Cn-binding MSCRAMM containing an N-terminal A domain, followed by 1−4 B repeats, the cell wall anchoring region, a transmembrane segment, and a short cytoplasmic tail. The A domain consists of three subdomains named N1, N2, and N3.[1] The segment of Cna showing the highest affinity for Cn is composed of the N1N2 subdomains, each adopting a variant of the IgG-like fold, which is composed of two antiparallel β-sheets and two α-helices.[2] Cn-binding is achieved through the high-affinity "collagen hug" mechanism, where the N1 and N2 subdomains cooperate to wrap around the rope-like structure of collagen.[2] Recent experiments have shown that the Cna−Cn bond is very strong (>1 nN) and that the B-region has a mechanical function that is essential for strong ligand binding.[3] The importance of the Cna−Cn interaction by *S. aureus* has been demonstrated in experimental arthritis,[4] and the potential of Cna as a virulence factor has been directly related to the adhesin's affinity for Cn.[5] Furthermore, vaccination with a recombinant fragment of Cna protects mice against sepsis-induced death.[6] Cna also contributes to the pathogenesis of

Received: December 15, 2016
Accepted: January 30, 2017
Published: February 2, 2017

DOI: 10.1021/acsnano.6b08404
ACS Nano 2017, 11, 2160−2170

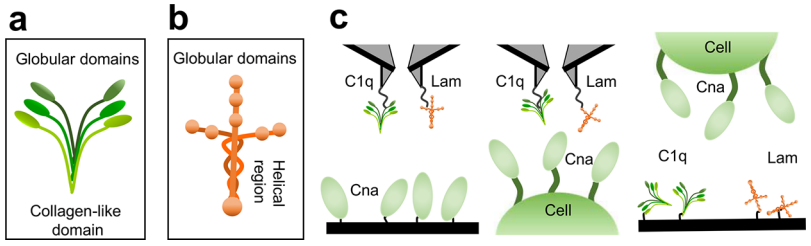

Figure 1. Force spectroscopy of Cna−C1q and Cna−Lam interactions. (a, b) Structures of the C1q (a) and Lam (b) proteins (see text for details). (c) AFM experiments (from left to right): SMFS using AFM tips functionalized with ligands and recombinant CNA_{31-344} or full length Cna expressed in *S. aureus* Phillips bacteria; SCFS of the interaction between *S. aureus* Phillips bacteria and ligand-coated substrates.

osteomyelitis and is involved in *S. aureus* infection of the cornea.[7,8]

Cna was also shown to bind to complement protein C1q and to inhibit the complement activation *via* the classical pathway (CP).[9] C1q is a 460 kDa glycoprotein composed of six heterotrimeric polypeptides, each consisting of six collagen-like stalks linked to six globular heads by a central fibril-like region (Figure 1a). The globular head region of C1q contains the antibody recognition site, while individual collagenous stalks interact with heterotetramer C1r2C1s2 to form the C1 complex which is the central component of the classical complement pathway. While molecular analyses suggested that Cna binds the collagenous domains of C1q,[9] whether this is achieved through a high-affinity hug-like mechanism is unclear.

Currently, it is not known whether Cna is capable of recognizing the matrix protein Lam, a key component of the basement membrane. Lam is a heterotrimer consisting of α-, β-, and γ- polypeptides that form an asymmetrical cruciform structure with the long arm comprising a Cn-like triple helix (Figure 1b). There have been several preliminary reports that hint at *S. aureus* binding to Lam.[10,11] In addition, the Cn-binding protein Ace from *Enterococcus faecalis*, which is structurally similar to Cna and interacts with Cn by the hug mechanism,[12] can also bind Lam.[13] Accordingly, while the functional roles of Cna in bacterial adhesion[14,15] and immune evasion[9] are established, its binding mechanisms are not fully understood. This prompted us to explore the molecular forces driving the interaction of Cna with C1q and Lam, using atomic force microscopy (AFM) techniques (Figure 1c).[16] The results show that Cna specifically binds to C1q and Lam through forces that are much weaker than those of the Cna−Cn bond, implying these bonds do not involve a high-affinity mechanism like the collagen hug. This finding emphasizes that Cna is engaged in various ligand-binding mechanisms, thus rationalizing its multiple functional roles during pathogenesis. In addition, monoclonal antibodies (mAbs) directed against the minimal Cn-binding domain of Cna are capable of efficiently blocking C1q and Lam-mediated adhesion. Our study demonstrates the power of force nanoscopy for identifying functions and binding mechanisms in staphylococcal adhesion proteins and for screening anti-adhesion compounds.

RESULTS AND DISCUSSION

Cna Specifically Binds to Collagen, C1q, and Laminin.

Prior to AFM analysis, we studied the ability of Cna to mediate bacterial attachment to ligand-coated substrates, using the *S. aureus* strain Phillips (here after $Cna^{(+)}$ cells), a clinical isolate from an osteomyelitis patient that expresses full length Cna.[4] Optical microscopy images showed that $Cna^{(+)}$ cells adhered strongly to C1q and Lam surfaces, whereas cells from the Cna deletion mutant ($Cna^{(-)}$ cells) did not (Figure 2). Previously, we made similar observations for Cn-coated substrates.[3] We

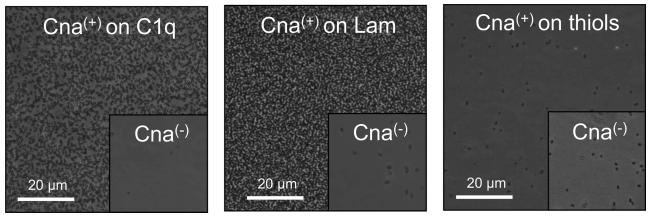

Figure 2. Bacterial adhesion to C1q and laminin. Optical microscopy images of *S. aureus* Phillips bacteria expressing full length Cna ($Cna^{(+)}$ cells) or not (insets, $Cna^{(-)}$ cells), adhering to C1q, Lam, and alkanethiol-coated substrates.

note that $Cna^{(+)}$ cells adhered poorly to alkanethiol monolayers, further supporting the specificity of bacterial adhesion (Figure 2).

These microscopic observations were found to correlate with macroscopic microtiter well assays. As can be seen in Figure 3a, $Cna^{(+)}$ cells attached to increasing amounts of C1q, Lam, and Cn adsorbed on the wells. The lack of adhesion of $Cna^{(+)}$ cells to bovine serum albumin (BSA) indicates that the Cna-mediated attachment to the different ligands is a specific process. To study Cna-dependent adhesion in the absence of other staphylococcal molecules, we analyzed the ability of a recombinant Cna fragment to bind Cn, C1q, and Lam using an enzyme-linked immunosorbent assay (ELISA). A fragment corresponding to the predicted N1N2 combination of subdomains (amino acid residues 31−344, hereafter CNA_{31-344}) was found to bind to microtiter wells coated with Cn, C1q, and Lam, in a dose-dependent and saturable manner (Figure 3b). From the saturation kinetics, the dissociation constant K_D of soluble Cna for Cn, C1q, and Lam was calculated and found to be 53 nM, 1.0 μM, and 2.2 μM, respectively. The Cn value is in the range of that estimated earlier by Kang *et al.*,[9] *i.e.*, 91 nM. We also probed the CNA_{31-344}−C1q and CNA_{31-344}−Lam interactions by surface plasmon resonance (SPR) by immobilizing C1q and Lam on a chip and injecting recombinant CNA_{31-344} in the mobile phase (Figure 3c−f). The best fit of the data points was obtained with the Langmuir isotherm equation describing the one-site binding model. From this we estimated K_D values of 21 ± 3.7 μM and 560 ± 33 nM for the CNA_{31-344}−C1q and CNA_{31-344}−Lam bonds, which are clearly higher than the 91 nM SPR value reported for Cn.[9] These observations show that the N1N2 subdomains of Cna bind to C1q and Lam with an affinity lower than that of the collagen hug interaction.

DOI: 10.1021/acsnano.6b08404
ACS Nano 2017, 11, 2160−2170

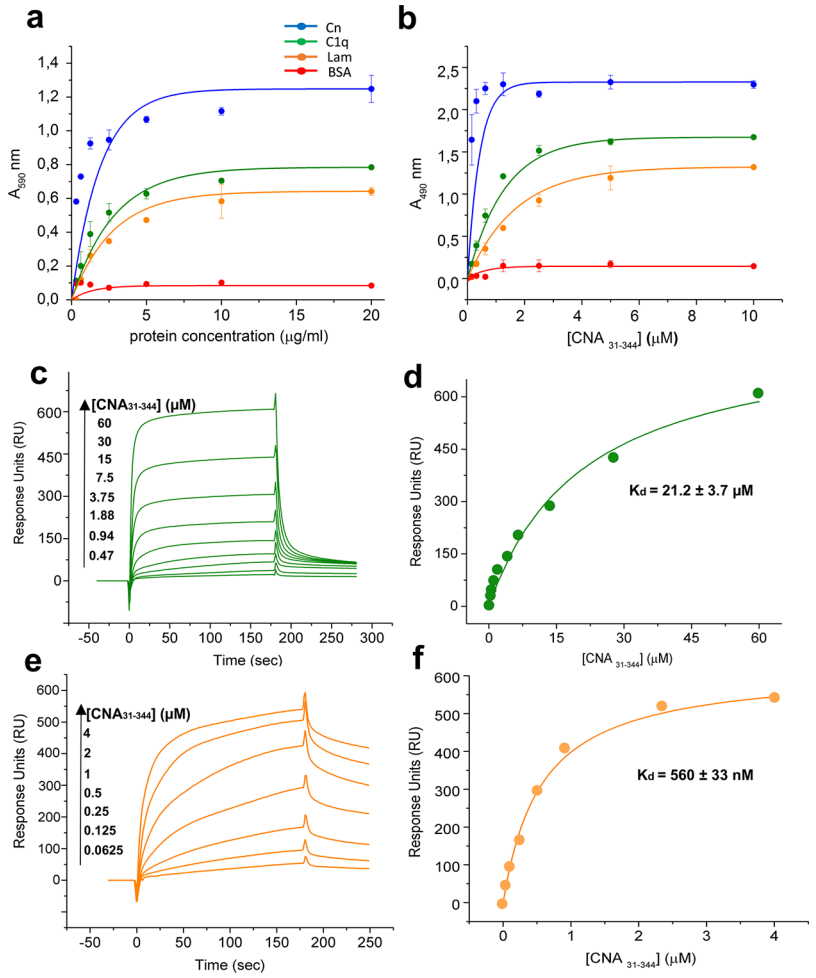

Figure 3. Binding of Cna to collagen, C1q, and laminin. (a) Macroscopic assay showing the adhesion of Cna$^{(+)}$ cells to increasing amounts of BSA, C1q, Lam, and Cn adsorbed on microtiter wells. After washing, attached bacteria were detected by crystal violet staining. (b) ELISA revealing the ability of the predicted N1N2 subdomain of Cna (CNA_{31-344}) to bind to microtiter wells coated with BSA, type II Cn, C1q, and Lam. The data points in (a) and (b) are the means and SD of three independent experiments each performed in triplicate. (c–f) SPR analysis of the CNA_{31-344}–C1q and CNA_{31-344}–Lam interactions: (c, e) sensograms showing the binding of CNA_{31-344} to C1q (c) or Lam (e) immobilized on a CM5 sensor chip; (d, f) plots of RU_{max} *vs* CNA_{31-344} concentrations. The data points were fitted with the Langmuir equation describing a 1:1 binding model. In each case, the figures show representative plots out of three experiments.

Strength of Single Cna–C1q and Cna–Lam Bonds. In light of the above results, we postulated that Cna is a multifunctional adhesin capable of binding to Cn, C1q, and Lam using the same subdomains but through different mechanisms. To test this hypothesis, we measured the strength of C1q or Lam interactions, at the single-molecule and single-cell levels (Figure 1c). We first used single-molecule force spectroscopy (SMFS; Figure 1c, left cartoon) to study the binding strength of CNA_{31-344} with C1q and Lam. To probe single molecules, ligands were attached to AFM tips using a PEG-benzaldehyde linker, whereas CNA_{31-344} was immobilized on solid substrates using *N*-hydroxysuccinimide (NHS). In Figure 4 we report the adhesion forces, rupture lengths, and typical retraction force curves obtained for the C1q and Lam interactions (n = 6144 forces curves using 3 different tips and substrates for C1q; n = 7139 force curves using 4 different tips and substrates for Lam). About half of the force curves displayed adhesion events with a mean adhesion force of 158 ± 29 pN (mean ± SD) and a rupture length of 29 ± 7 nm for C1q and 185 ± 83 pN and 28 ± 8 nm for Lam. The rupture values, ∼30 nm, are shorter than the length of fully extended CNA_{31-344} molecules, ∼100 nm,[3] indicating that the N1N2 subdomains are not (or only partially) unfolded. Force curves were also acquired at various loading rates (Figure 4c,f). The effective loading rate was estimated from the force *vs* time curves.[17] As expected for specific biomolecular bonds, the mean adhesion force (F) increased linearly with the logarithm of the loading rate (r), for both C1q (Figure 4c) and Lam (Figure 4f). The kinetic off-rate constant of dissociation at zero force was obtained by extrapolation to zero force,[3] k_{off} = 0.3 s^{-1} and 0.4 s^{-1}. These values indicate that bond dissociation is fast, which does not support a high affinity binding mechanism.

We then asked whether the binding strength of CNA_{31-344} might differ from that of the entire Cna protein. Recent AFM experiments using bacterial cells expressing full length Cna revealed that the B-region of Cna plays a role in favoring strong attachment to Cn substrates.[3] A model was proposed where the B-region helps in projecting the A-region away from the bacterial surface, enabling the multiple conformational changes needed for the hug complex to form. To test whether the B-region plays a similar functional role in C1q and Lam interactions, we measured the binding strength of full length Cna on living bacteria, using C1q and Lam-terminated tips (Figure 1c, middle panel). The SMFS experiments presented in

DOI: 10.1021/acsnano.6b08404
ACS Nano 2017, 11, 2160–2170

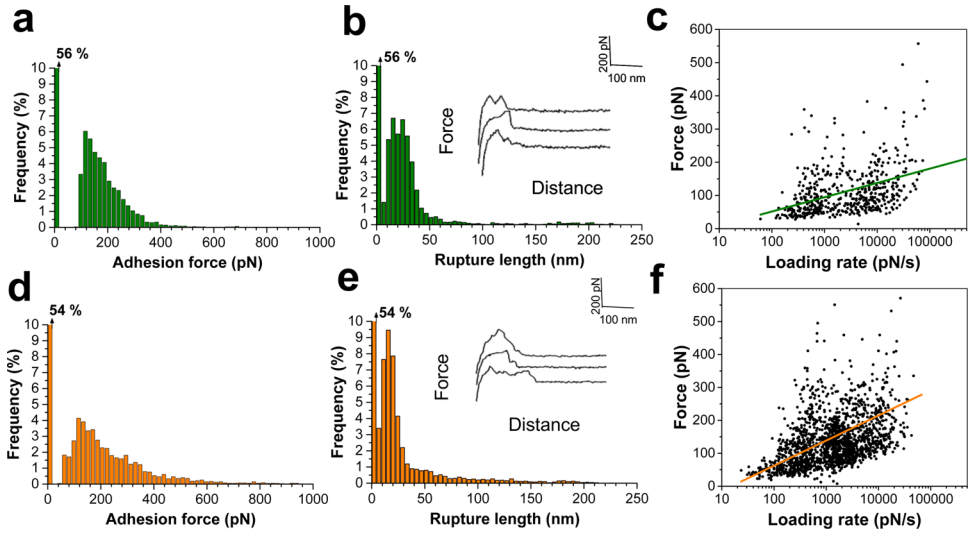

Figure 4. Binding strength of recombinant CNA_{31-344} with C1q and Lam. (a, d) Adhesion force histograms and (b, e) rupture length histograms with representative retraction force profiles obtained by recording force−distance curves in PBS between tips functionalized with C1q (a, b) or Lam (d, e), and CNA_{31-344} substrates. Data were pooled from independents experiments using 3 different tips and substrates for C1q and for Lam. All curves were obtained using a contact time of 100 ms, a maximum applied force of 250 pN, and approach and retraction speeds of 1000 nm s^{-1}. (c, f) Dependence of the adhesion force on the loading rate applied during retraction, measured using 3 different tips and substrates for C1q and for Lam, using a contact time of 100 ms, a maximum applied force of 250 pN, and an approach speed of 1000 nm s^{-1}.

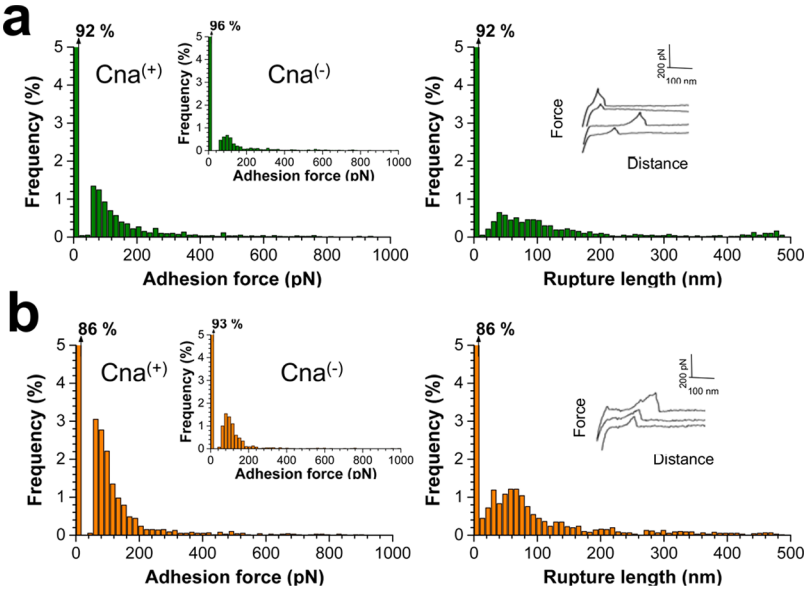

Figure 5. Strength of single Cna−C1q and Cna−Lam bonds in living bacteria. (a, b) Adhesion force (left) and rupture length (right) histograms with representative retraction force profiles obtained by recording force−distance curves in PBS between C1q tips and 10 different $Cna^{(+)}$ cells (a) or Lam tips and 9 different $Cna^{(+)}$ cells (b). The insets show the data obtained in the same conditions for 10 and 9 $Cna^{(-)}$ cells. All curves were obtained using a contact time of 100 ms, a maximum applied force of 250 pN, and approach and retraction speeds of 1000 nm s^{-1}.

Figure 5 show that the curves on $Cna^{(+)}$ cells featured adhesion peaks of 197 ± 84 pN and 158 ± 59 pN and 139 ± 91 nm and 139 ± 80 nm extensions for C1q and Lam bonds, respectively (from a total of n = 10,240 curves from 10 different tips and cells for C1q and 9216 curves from 9 different tips and cells for Lam). $Cna^{(-)}$ cells showed a lower adhesion frequency (insets), yet adhesion was not completely abolished. The moderate forces, in the range of those measured for CNA_{31-344}, are in sharp contrast with the strong force (~1200 pN) of the high affinity collagen hug interaction.[3] These observations lead us to conclude (i) that C1q and Lam interactions have moderate strength and do not involve a high affinity, hug-like mechanism and (ii) that the B-region of Cna plays no (or only a minor) role in these interactions.

Forces in Single-Cell Adhesion. To further explore the mechanisms of Cna-mediated adhesion, we measured the forces between whole bacteria and protein-coated substrates using single-cell force spectroscopy (SCFS, Figure 1c, right panel). Living *S. aureus* cells were immobilized on to AFM cantilevers, and force−distance curves were recorded between the bacterial

DOI: 10.1021/acsnano.6b08404
ACS Nano 2017, 11, 2160−2170

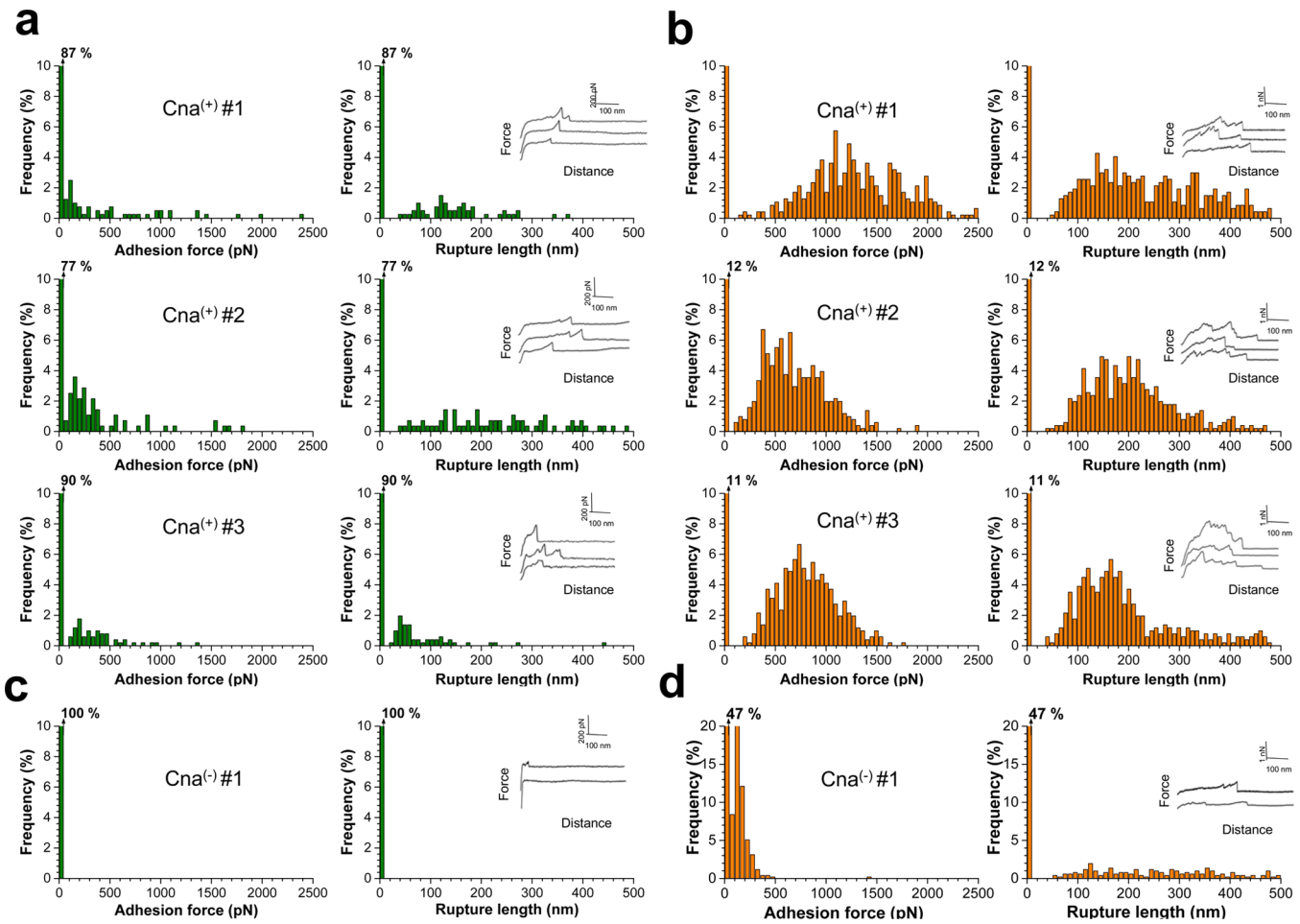

Figure 6. Forces driving single-cell adhesion to C1q and Lam substrates. (a, b) Adhesion force (left) and rupture length (right) histograms with representative retraction force profiles obtained by recording force–distance curves in PBS between three different Cna$^{(+)}$ cells and C1q-substrates (a) or Lam-substrates (b). (c, d) Force data obtained in the same conditions for a Cna$^{(-)}$ cell. All curves were obtained using a contact time of 100 ms, a maximum applied force of 250 pN, and approach and retraction speeds of 1000 nm s^{-1}.

probes and C1q or Lam substrates. In Figure 6a,b we present the adhesion forces and rupture lengths measured for three Cna$^{(+)}$ cells (including cells from independent cultures; for more cells see Table 1). For both substrates, variations were observed from one cell to another, but the overall shapes of the force curves were generally similar for a given ligand.

On C1q, the adhesion probability was moderate (16 ± 19%), and the curves generally showed single or double well-defined adhesion peaks of 325 ± 231 pN magnitude and 139 ± 101 nm extension (mean ± SD, n = 9728 force curves from 18 cells). By contrast, on Lam, a higher adhesion probability (65 ± 28%) was observed. Also, adhesion forces and rupture lengths were larger (742 ± 412 pN and 333 ± 146 nm, n = 9728 curves from 18 cells), and the adhesion profiles featured complex shapes with multiple ruptures. We believe that these features mostly reflect specific Cna-mediated interactions as they were missing—or strongly inhibited—in Cna$^{(-)}$ cells (Figure 6c,d). Supporting the validity of our measurements, we find it remarkable that results obtained on two different instruments were in good agreement (Table 1). The rupture lengths of the C1q interactions are much smaller than the length of the fully extended Cna molecule (~340 nm) indicating that the protein is too rigid to be unfolded. Isopeptide bonds in the B domain of Cna[18] may play a role in stabilizing the protein structure.

Comparison of SCFS and SMFS experiments shows that the adhesion strength of single Cna$^{(+)}$ cells to C1q substrates was not that much higher than that of single CNA$_{31-344}$ proteins, suggesting that the adhesion of whole cells involved only one (two) molecular bond(s). However, on Lam the strength of single-cell adhesion was clearly higher than that of single proteins and showed multiple ruptures, implying that the cell–Lam interaction involves multiple bonds. It is tempting to speculate that bacterial adhesion to Lam might be enhanced by cooperative binding of multiple Cna–Lam molecular complexes. Yet it is also possible that a single Cna protein contains more than one adhesion site and might be able to bind to multiple ligands or that Lam has multiple sites capable to bind several Cna proteins. Further work is needed to establish whether such cooperative or multivalent interactions play a role in bacterial adhesion to Lam.

A major finding of this study is that the C1q and Lam adhesive interactions markedly differed from the Cn interaction. We recently showed (i) that bacterial adhesion to Cn involves well-defined, linear adhesion peaks with very strong forces (in the nN range), consistent with the high-affinity collagen hug mechanism and (ii) that the B-region of Cna is required for strong ligand binding. These features were missing in C1q and Lam interactions, indicating that their molecular origin is different from the Cn interaction.

DOI: 10.1021/acsnano.6b08404
ACS Nano 2017, 11, 2160–2170

Table 1. Probability of Adhesion (P_{adh}), Maximum Adhesion force (F_{adh}), and Rupture Length (L_{rupt}) Measured by SCFS between Cna$^{(+)}$ or Cna$^{(-)}$ Cells and C1q or Lam Substrates

		C1q			laminin		
		P_{adh} (%)[a]	F_{adh} (pN)	L_{rupt} (nm)	P_{adh} (%)	F_{adh} (pN)	L_{rupt} (nm)
Cna$^{(+)}$	cell1[b]	–	–	–	40	1648 ± 132	326 ± 14
	cell2[b]	26	772 ± 28	100 ± 3	41	1089 ± 61	429 ± 10
	cell3[b]	71	734 ± 13	334 ± 70	26	927 ± 69	483 ± 27
	cell4[b]	7	242 ± 31	311 ± 32	74	877 ± 16	532 ± 11
	cell5[b]	10	278 ± 29	199 ± 12	–	–	–
	cell6[b]	0	–	–	45	416 ± 17	356 ± 12
	cell7[b]	54	135 ± 4	249 ± 16	–	–	–
	cell8[b]	4	74 ± 8	168 ± 39	86	362 ± 18	278 ± 10
	cell9[b]	35	166 ± 6	147 ± 20	75	380 ± 18	415 ± 11
	cell10[b]	0	–	–	–	–	–
	mean[b]	**23 ± 8**	**291 ± 97**	**167 ± 40**	**55 ± 8**	**814 ± 179**	**402 ± 34**
	cell1[c]	17	473 ± 49	152 ± 11	0	–	–
	cell2[c]	13	271 ± 34	271 ± 34	100	1092 ± 33	526 ± 16
	cell3[c]	10	391 ± 37	86 ± 10	71	415 ± 13	275 ± 9
	cell4[c]	9	356 ± 56	59 ± 5	90	1335 ± 27	235 ± 5
	cell5[c]	11	284 ± 42	75 ± 19	88	695 ± 15	206 ± 4
	cell6[c]	3	490 ± 40	52 ± 3	23	332 ± 17	99 ± 5
	cell7[c]	1	280 ± 99	46 ± 1	22	252 ± 15	71 ± 5
	cell8[c]	8	232 ± 24	96 ± 7	89	654 ± 11	191 ± 5
	cell9[c]	5	680 ± 150	151 ± 16	78	463 ± 30	494 ± 11
	cell10[c]	–	–	–	100	403 ± 7	411 ± 5
	mean[c]	**8 ± 2**	**384 ± 48**	**110 ± 24**	**73 ± 10**	**627 ± 122**	**279 ± 55**
	mean[b]+[c]	**16 ± 5**	**325 ± 54**	**139 ± 24**	**65 ± 7**	**742 ± 103**	**333 ± 37**
Cna$^{(-)}$	cell1[b]	0			49	189 ± 9	392 ± 9
	cell2[b]	0			72	190 ± 6	412 ± 11
	cell3[b]	0			65	205 ± 5	470 ± 12
	cell4[b]	0			65	152 ± 3	312 ± 12
	cell5[b]	0			53	160 ± 6	322 ± 15
	cell6[b]	0			0	–	–
	cell7[b]	0			8	229 ± 22	103 ± 16
	cell8[b]	0			8	181 ± 16	91 ± 8
	cell9[b]	0			2	46 ± 5	78 ± 10
	cell10[b]	0			3	50 ± 4	64 ± 10
	mean	**0**	**0**	**0**	**33 ± 10**	**140 ± 25**	**224 ± 55**

[a]P_{adh} = % of curves with adhesion forces. [b]Data acquired with a JPK instrument. [c]Data acquired with a Bruker instrument.

Consistent with this, K_D values obtained by ELISA and SPR—here and in earlier experiments[9]—indicate that Cna binds C1q and Lam with lower affinity than Cn. That the B-region does not seem to play a role in activating C1q and Lam interactions further supports the notion that they do not involve the multiple conformational changes of the classical hug mechanism. All together, these observations demonstrate that Cna is a multifunctional adhesin capable of binding to Cn, C1q, and Lam using the same subdomains but through different binding mechanisms.

Blocking *S. aureus* Adhesion to C1q and Lam Using Antibodies. In a previous study, conformational mAbs were raised against the recombinant minimal Cn-binding region of Cna, $CNA_{151-318}$.[19] These mAbs were able to inhibit ^{125}I-collagen binding to $CNA_{151-318}$ as well as to intact *S. aureus* cells. They also interfered with the attachment of bacteria to Cn substrates. As Cn, C1q, and Lam interactions involve the same region of Cna, we hypothesized that mAbs directed against the Cn-binding domain might efficiently block the adhesion of *S. aureus* to C1q and Lam substrates. To test this idea, we studied the influence of mAb 9G7 on single-cell adhesion using SCFS. In Figure 7a,b, it can be seen that for many cells, addition of 9G7 dramatically decreased the adhesion probability toward C1q and Lam substrates. The control mAb 16H9 that does not recognize the ligand-binding region did not substantially change the adhesion probability. There were variations from one cell to another, and the blocking efficiency depended on the initial binding probability. Poor blocking was observed on Lam substrates for cells exhibiting a very high (>90%) binding probability. This low efficiency could reflect the notion that when cells are engaged in many Cna-mediated interactions, possibly cooperative or multivalent interactions, only a fraction of the adhesins are inhibited, and therefore the cells remain sticky. Despite the observed variability, we estimate that the concentration required to inhibit 50% of maximum binding (IC_{50}) was in the range of ~1 μg mL^{-1} for C1q and ~5 μg mL^{-1} for Lam.

These single-cell analyses were combined with ELISA assays. Microtiter wells were coated with C1q, Lam, and Cn for comparison and examined for attachment of *S. aureus* Phillips in the presence of increasing concentrations of 9G7 (Figure 7c–e). This mAb completely blocked adherence of bacteria to Lam and Cn when added at 0.3–0.6 μg/well. Conversely, a maximal inhibitory effect of only 60% on bacterial attachment was

DOI: 10.1021/acsnano.6b08404
ACS Nano 2017, 11, 2160–2170

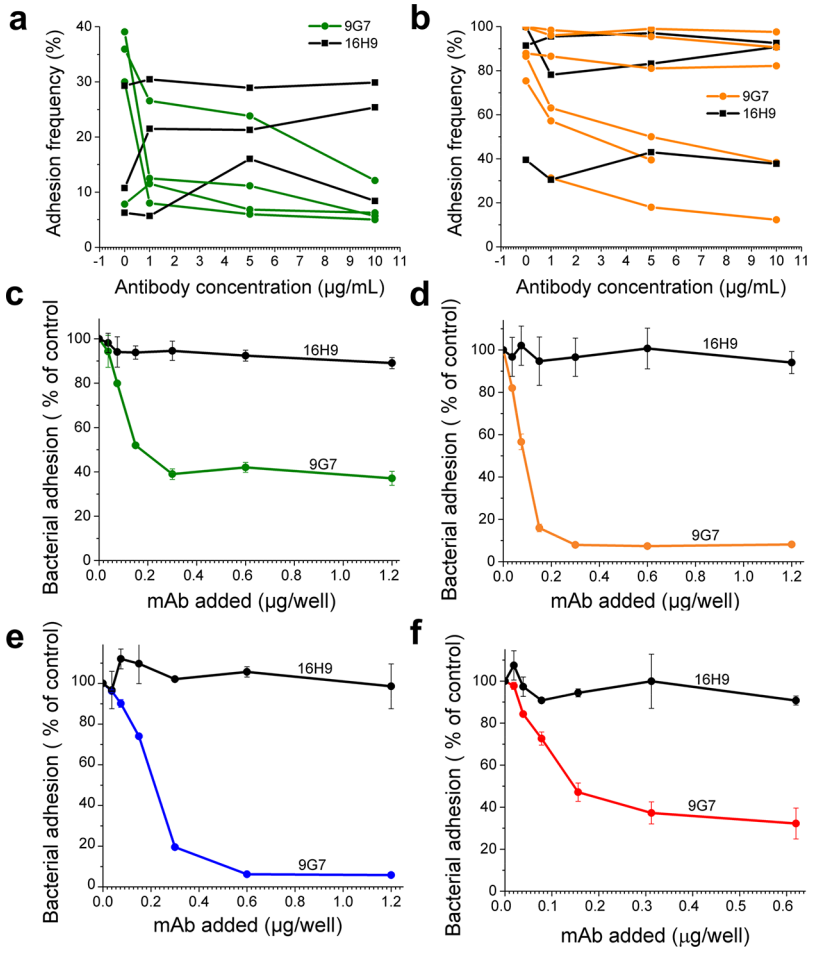

Figure 7. Blocking *S. aureus* adhesion to C1q and Lam using antibodies. (a, b) Concentration-dependent effects of mAbs 9G7 and 16H9 on the probability of adhesion between Cna$^{(+)}$ cells and C1q (a) or Lam (b) substrates. (c–f) Macroscale assay of the blocking activity of mAbs 9G7 and 16H9. Bacteria were added to microtiter plate wells coated with C1q (c), Lam (d), Cn (e), and Matrigel matrix (f). Adherence was measured using crystal violet staining. Data are expressed as percentage of a control, *i.e.*, incubation performed in the absence of any potential inhibitor. The data points are the means and SD of three independent experiments each performed in triplicate.

observed with C1q. In all cases, no effect was observed with the control mAb 16H9. We further tested the blocking activity of mAbs using Matrigel, a commercial solubilized basement membrane preparation extracted from Engelbreth–Holm–Swarm mouse sarcoma mainly composed of Lam, Cn type IV, heparan sulfate proteoglycans and nidogen. Bacterial adhesion to wells coated with Matrigel showed that bacteria strongly attached to the immobilized substrate. Upon addition of mAb 9G7, an inhibition effect >70% was achieved at 0.3 μg/well (Figure 7f). The control mAb 16H9 had no effect on the bacteria–Matrigel interaction. These nanoscopic and macroscopic assays show that 9G7 interferes with bacterial adhesion to C1q and Cna substrates and also to more biologically relevant basement membranes, suggesting this mAb acts as a competitive inhibitor by binding Cna residues that are in direct contact with C1q and Lam ligands.

CONCLUSIONS

The *S. aureus* surface protein Cna mediates bacterial adhesion to Cn through strong molecular bonds,[3] formed *via* the high-affinity multistep collagen hug mechanism.[2] Here we have employed single-molecule and single-cell experiments to show that Cna also mediates attachment to C1q and Lam, through binding mechanisms that differ from the classical collagen hug. C1q and Lam interactions are mediated by the N1N2 subdomains of Cna, do not require the B-region, and are much weaker than the high affinity Cn interaction. C1q and Lam-binding can be successfully blocked by mAbs against the minimal binding domain of Cna. This leads us to conclude that Cna is a multifunctional adhesin capable of binding to Cn, C1q, and Lam using the same subdomains but through different binding mechanisms. This study represents a significant step forward in the development of nanoscopy techniques for studying the multifunctionality of staphylococcal adhesins and for the label-free screening of anti-adhesion agents.

An important outcome of our work is that the forces driving the Cna–C1q and Cna–Lam interactions are dramatically different from the Cna–Cn interaction forces. Previous AFM experiments showed that the high-affinity collagen hug bond is remarkably strong (~1200 pN) and requires the B repeats of Cna, thus indicating that CNA_{31-344} alone is not sufficient to give rise to strong interactions.[3] The B-region features spring-like properties that are believed to provide a means to project the protein binding sites away from the crowded cell surface environment and to favor the multiple conformational changes needed for forming collagen hug complexes. By contrast, C1q and Lam interactions have moderate strength (~200 pN) and

DOI: 10.1021/acsnano.6b08404
ACS Nano 2017, 11, 2160–2170

do not require the B-region, meaning it plays no (or a minor) role in activating C1q and Lam interactions.

Our C1q results are consistent with the findings of Kang *et al.*,[9] showing that Cna binds to a collagenous domain of C1q with a much lower affinity than Cn. They reported that mutants in the recombinant Cna protein with substitutions in the Cn binding loop between N1 and N2, and in the latching peptide, have similar relative reductions in binding affinity to C1q and Cn measured by SPR and ELISA. It is therefore tempting to suggest that elements of the hug mechanism might be used, but the full hug is not formed because of structural differences between Cn and C1q. In line with this notion, the Cn-like domain of C1q is a hexamer, while Cn is a triple helix. As for the Lam-binding activity of Cna, it is not known which region of Lam is involved in the interaction. Cna may bind to the long triple helix of Lam, which resembles the structure of the Cn molecule. Here also our AFM, ELISA, and SPR data suggest that the first step of the hug mechanism (binding into the Cna trench) is used, but the subsequent steps leading to high affinity complexes cannot be achieved due to differences in the Lam and Cn structures. Whereas bacterial adhesion to C1q-substrates involves very few molecular bonds, adhesion to Lam is mediated by multiple bonds. The moderate unit binding force of Cna might be amplified by multivalent or cooperative bonds that would enhance the strength and duration of the bacterial–substrate interaction. C1q and Lam-mediated adhesion can be efficiently blocked by mAbs directed against the minimal binding domain of Cna, suggesting they could be used as competitive inhibitors of C1q and Lam in future medical applications. Collectively, our findings emphasize the multiple functions and binding mechanisms of the N1N2 subdomains of Cna.

We believe that the ability of Cna to bind C1q and Lam is of biological significance. C1q binding to Cna results in the inhibition of its interaction with C1r. As a result, $C1r_2C1s_2$ is displaced from C1q, and C1 complex formation is blocked, and activation of the CP of the complement is not allowed. Thus, Cna may be an additional important component of a more general evasion strategy of this remarkable pathogen.[9] The ability of Cn-binding proteins to bind Lam is consistent with earlier reports. Several bacterial MSCRAMMs from different species share the ability to interact with both Cn and Lam and/or other extracellular matrix components, including ACE of *Streptococcus faecalis*,[13] the outer membrane lollipop-like protein YadA of *Yersinia enterocolitica*,[20−22] and the Fnm from *Enterococcus faecium*.[23] Notably, ACE and Cna A domains have similar secondary structures and both proteins bound at multiple sites in type I collagen with micromolar affinities.[24] Furthermore, ACE binds Cn by the hug model.[12] We speculate that the proposed trench on the ACE and Cna A domains, which has been implicated in binding the triple helix Cn structure, might also responsible for binding the rigid triple helix structure of the Lam long arm. By analogy, in the mammalian kingdom, the Cn-binding integrins $\alpha_1\beta_1$ and $\alpha_2\beta_1$, both of which contain a trench in the binding domain, have been shown to bind Lam in addition to several types of collagens.[25,26] Interestingly, although Cna and these integrins have unrelated amino acid sequences and secondary structure composition, they recognize Cn *via* a similar mechanism.[27] So it seems that adhesins from various organisms have evolved similarly, providing them with remarkable multifunctional binding properties.

METHODS

Bacterial Strains and Cultures. The *S. aureus* strain Phillips ($Cna^{(+)}$ cells) used in this study was originally isolated from a patient diagnosed with osteomyelitis. Its isogenic collagen adhesin-negative mutant is PH100 $Cna^{(-)}$.[3] Cells were grown in tryptic soy broth (TSB) to the stationary phase (16–18 h) and harvested by centrifugation 3 min at 2500 x *g* and washed 2 times in phosphate-buffered saline (PBS) buffer.

C1q, Laminin, Recombinant Cna, and Monoclonal Antibodies. C1q was purchased from Complement Technology Inc. (Texas, USA). Ultrapure laminin (Engelbreth–Holm–Swarm murine sarcoma basement membrane) was purchased from Sigma. CNA_{31-344} and monoclonal antibodies 9G7 and 16H9 raised against recombinant $CNA_{151-318}$ were produced as previously reported.[3]

Microtiter Plate Cell Adhesion Assay. Attachment of *S. aureus* Phillips to immobilized Cn, C1q, and Lam was determined as reported earlier.[28] Briefly, microtiter plates were coated with doubling dilutions of Cn type II, C1q, Lam, or BSA in 0.1 M sodium carbonate, pH 9.5 overnight at 4 °C. The plates were washed with 0.5% (v/v) Tween 20 in PBS (PBST). To block additional protein-binding sites, the wells were treated for 1 h at 22 °C with BSA (2% v:v) in PBS. The plates were washed three times with PBS. 100 μL of *S. aureus* Phillips cells (OD = 2.0) were added to each well and incubated for 90 min at 37 °C. Wells were washed three times with PBS, and bound cells were fixed for 20 min with formaldehyde (4%, v/v) and stained with 100 μL of crystal violet (0.5% v/v) for 1–2 min. After washing, 50 μL of 10% acetic acid was added to each well, and the absorbance was measured at 590 nm using an ELISA plate reader.

Binding of Recombinant Cna to Cn, C1q, and Lam by ELISA. The ability of CNA_{31-344} to bind Cn, C1q, Lam, or BSA was determined using ELISA. Microtiter wells were coated overnight at 4 °C with 1 μg/well of each protein in 0.1 M sodium carbonate, pH 9.5. The plates were washed with 0.5% (v/v) Tween 20 in PBS (PBST). To block additional protein-binding sites, the wells were treated for 1 h at 22 °C with BSA (2% v/v) in phosphate-buffered saline (PBS). The plates were then incubated for 1 h with the appropriate amounts of CNA_{31-344}. After several washings with PBST, 100 μL of the anti-Cna mouse serum diluted 1:2000 in BSA (1% v/v) was added to the wells and incubated for 90 min. The plates were washed and then incubated for 1 h with HRP-conjugated antimouse IgG diluted 1:1000. After washing, *o*-phenylenediamine dihydrochloride was added, and the absorbance at 490 nm was determined using an ELISA plate reader (Bio-Rad). To calculate the relative affinity associative constant (K_A) value, the data were fitted using the following equation: $A = A_{max}[L]K_A/1 + K_A[L]$, where $[L]$ is the molar concentration of the ligand (Cna). The reported dissociation contanst (K_D) value was calculated as the reciprocal of K_A.

Surface Plasmon Resonance. SPR analyses were carried out using a multicycle injection strategy on a dual flowcell Biacore-X100 instrument (GE-Healthcare). Each binding curve was subtracted from the corresponding baseline, accounting for nonspecific binding (<2% of RU_{max}), and the data were analyzed using the BIAevaluation software. Commercial purified Lam (Sigma) or C1q (Complement Technology Inc.) were immobilized on a carboxymethylated-dextran chip (CM5), and increasing concentrations of recombinant CNA_{31-344} solutions were injected in the mobile phase. The

DOI: 10.1021/acsnano.6b08404
ACS Nano 2017, 11, 2160–2170

dissociation constant (K_D) of the CNA_{31-344}-Lam or CNA_{31-344}−C1q complex was determined in the affinity mode, by plotting the value of RU_{max}, measured at the steady state, as a function of [CNA_{31-344}] and fitting the data points to the Langmuir equation describing a 1:1 binding model. SPR measurements were carried out in HBS, containing 3 mM EDTA and 0.05% polyoxyethylene sorbitan (HBS-EP$^+$).

C1q, Lam, and CNA_{31-344}-Coated Substrates. To prepare functionalized substrates for microscopic adhesion and SCFS and SMFS experiments, gold-coated glass coverslips were immersed overnight in an ethanol solution containing 1 mM of 10% 16-mercaptododecahexanoic acid/90% 1-mercapto-1-undecanol (Sigma), rinsed with ethanol, and dried with N_2. Substrates were then immersed for 30 min into a solution containing 10 mg·mL^{-1} *N*-hydroxysuccinimide (NHS) and 25 mg·mL^{-1} 1-ethyl-3-(3-(dimethylamino)propyl)-carbodiimide (EDC) (Sigma), rinsed with Ultrapure water (ELGA LabWater), incubated with 0.2 mg·mL^{-1} of proteins for 1 h, rinsed further with PBS buffer, and then immediately used without dewetting.

Microscopic Adherence Assays. A microscopic adhesion assay was used to assess bacterial adhesion on C1q and Lam substrates. Substrates were incubated for 2 h in 200 μL bacterial suspensions in PBS with an optical density at 590 nm of 1 (corresponding to a bacterial density of around 10^9 cells/mL). After 2 h, the substrates were gently rinsed by five consecutive washings in PBS and directly imaged using an inverted optical microscope (Zeiss axio Observer Z1) equipped with a Hamamatsu camera C10600. For comparison, we also analyzed bacterial adhesion onto alkanethiol-coated substrates.

Single-Molecule Force Spectroscopy. SMFS measurements were performed at room temperature (20 °C) in PBS buffer using a Nanoscope VIII Multimode AFM (Bruker corporation, Santa Barbara, USA). For experiments on model surfaces, oxide sharpened microfabricated Si_3Ni_4 cantilevers with a nominal spring constant of ∼0.01 N m^{-1} (MSCT, Microlevers, Bruker Corporation) were functionalized with C1q or Lam using PEG-benzaldehyde linkers, as described elsewhere.[3,29] The spring constants of the cantilevers were measured using the thermal noise method. Multiple force−distance curves were recorded on areas of 10 × 10 μm^2, using an applied force of 250 pN, a constant approach-retraction speed of 1 μm·s^{-1}, and a contact time of 100 ms.

For experiments on cell surfaces, gold cantilevers (OMCL-TR4, Olympus Ltd., Tokyo, Japan) with a nominal spring constant of ∼0.02 N m^{-1} were functionalized with C1q or Lam using the NHS chemistry as described above for substrates. The spring constants of the cantilevers were measured using the thermal noise method. Bacteria were immobilized by mechanical trapping into porous polycarbonate membranes (Millipore, Billerica, MA) with a pore diameter of 0.8 μm. After filtering a cell suspension, the membrane was rinsed with PBS, cut (1 × 1 cm^2), and attached to a steel sample puck using a small piece of double-faced adhesive tape. The mounted sample was transferred into the AFM liquid cell while avoiding dewetting. Bare tips were first used to localize and image individual cells and then replaced by functionalized tips. Adhesion maps were obtained by recording 1024 force−distance curves on areas of 500 × 500 nm^2, using an applied force of 250 pN, a constant approach-retraction speed of 1 μm·s^{-1}, and a contact time of 100 ms. SMFS data were analyzed using the Nanoscope Analysis software from Bruker (Santa Barbara, USA). Adhesion force and distance rupture histograms were obtained by calculating the adhesion force and rupture distance of the last peak for each curve. For each condition, experiments were repeated at least three times.

Single-Cell Force Spectroscopy. Bacterial cell probes were obtained as previously described.[3,30,31] SCFS measurements were then performed either with a Nanowizard III AFM (JPK Instruments, Germany) or with a Bioscope Catalyst AFM (Bruker Corporation, USA) equipped with a Zeiss Axio Observer Z1 and a Hamamatsu camera C10600. The nominal spring constant of the colloidal probe cantilever was ∼0.06 N·m^{-1}, as determined by the thermal noise method. 50 μL of diluted bacterial suspension (10^6 cells/mL) was deposited into a glass Petri dish containing C1q and laminin-coated substrates at a distinct location within the Petri dish. Three mL of PBS were added to immerse bacteria and functionalized substrates. The colloidal probe was brought into contact with an isolated bacterium and retracted to attach the bacterial cell; proper attachment of the cell on the colloidal probe was checked using optical microscopy. Cell probes were used to measure cell−substrates interaction forces at room temperature (20 °C), using an applied force of 250 pN, a constant approach-retraction speed of 1 μm·s^{-1}, and a contact time of 100 ms. Data were analyzed using either the Data Processing software from JPK Instruments (Berlin, Germany) or Nanoscope Analysis software from Bruker (Santa Barbara, USA). Adhesion force and distance rupture histograms were obtained by calculating the maximum adhesion force and rupture distance of the last peak for each curve. For each condition, experiments were repeated for at least five times. For blocking experiments, mAbs were added at increasing concentrations up to 10 μg·mL^{-1}, and the forces were measured after 15 min.

Effect of Antibodies on Bacterial Attachment Using Microtiter Plate Assays. The effect of anti-Cna mAbs 9G7 and 16H9 on the attachment of *S. aureus* Phillips to Cn, C1q, or Lam was examined by pre-incubating bacteria (OD = 2.0) with increasing amounts of the mAbs. 100 μL of the staphylococcal suspensions were then added to plates coated with 1 μg/well of each substrate, and the mixtures incubated for 90 min at 37 °C. Attachment of bacteria to the wells was determined by crystal violet staining as reported above. The effect of mAbs on bacterial adherence to Matrigel, a reconstituted basal membrane, was also investigated. Matrigel matrix (BD Bioscences, Ma, USA; protein content: ∼10 mg/mL) was diluted with ice-cold PBS to 0.1 mg/mL. Microtiter wells were coated overnight at 22 °C with 100 μL of the obtained solution. Attachment of *S. aureus* Phillips to the wells and the effect of mAbs were studied as described above.

AUTHOR INFORMATION

Corresponding Authors

*E-mail: Yves.Dufrene@uclouvain.be.
*E-mail: pspeziale@unipv.it.

ORCID

Giampiero Pietrocola: 0000-0002-7069-8155
Yves F. Dufrêne: 0000-0002-7289-4248

Author Contributions

[∇]These authors contributed equally. C.V., V.P., G.P., S.R., D.P., V.D.F., T.J.F., P.S., and Y.F.D. designed the experiments, analyzed the data, and wrote the article. C.V., V.P., G.P. and S.R. collected the data.

Notes

The authors declare no competing financial interest.

DOI: 10.1021/acsnano.6b08404
ACS Nano 2017, 11, 2160−2170

ACKNOWLEDGMENTS

Work at the Université catholique de Louvain was supported by the European Research Council (ERC) under the European Union's Horizon 2020 research and innovation programme (grant agreement no. 693630), the FNRS-WELBIO (grant no. WELBIO-CR-2015A-05), the National Fund for Scientific Research (FNRS), the Federal Office for Scientific, Technical and Cultural Affairs (Interuniversity Poles of Attraction Programme), and the Research Department of the Communauté française de Belgique (Concerted Research Action). Work at the University of Pavia was supported by the Fondazione CARIPLO (Grant Vaccines 2009-3546). Work at the University of Padua was supported in part by the PRAT-2015 Grant. Y.F.D. is Research Director at the FNRS. We thank David Alsteens for help with data treatment, Joan Geoghegan for contributing to the production of recombinant proteins, and Magnus Höök for providing us with the Phillips mutant strain.

REFERENCES

(1) Patti, J. M.; Boles, J. O.; Höök, M. Identification and Biochemical Characterization of the Ligand Binding Domain of the Collagen Adhesin from *Staphylococcus aureus*. *Biochemistry* **1993**, *32*, 11428−11435.

(2) Zong, Y.; Xu, Y.; Liang, X.; Keene, D. R.; Höök, A.; Gurusiddappa, S.; Narayana, S. V. L. A 'Collagen Hug'Model for *Staphylococcus aureus* CNA Binding to Collagen. *EMBO J.* **2005**, *24*, 4224−4236.

(3) Herman-Bausier, P.; Valotteau, C.; Pietrocola, G.; Rindi, S.; Alsteens, D.; Foster, T. J.; Speziale, P.; Dufrêne, Y. F. Mechanical Strength and Inhibition of the *Staphylococcus aureus* Collagen-Binding Protein Cna. *mBio* **2016**, *7*, e01529-16.

(4) Patti, J. M.; Bremell, T.; Krajewska-Pietrasik, D.; Abdelnour, A.; Tarkowski, A.; Rydén, C.; Höök, M. The *Staphylococcus aureus* Collagen Adhesin is a Virulence Determinant in Experimental Septic Arthritis. *Infect. Immun.* **1994**, *62*, 152−161.

(5) Xu, Y.; Rivas, J. M.; Brown, E. L.; Liang, X.; Höök, M. Virulence Potential of the Staphylococcal Adhesin CNA in Experimental Arthritis is Determined by Its Affinity for Collagen. *J. Infect. Dis.* **2004**, *189*, 2323−2333.

(6) Nilsson, I. M.; Patti, J. M.; Bremell, T.; Höök, M.; Tarkowski, A. Vaccination with a Recombinant Fragment of Collagen Adhesin Provides Protection Against *Staphylococcus aureus*-Mediated Septic Death. *J. Clin. Invest.* **1998**, *101*, 2640−2649.

(7) Elasri, M. O.; Thomas, J. R.; Skinner, R. A.; Blevins, J. S.; Beenken, K. E.; Nelson, C. L.; Smelter, M. S. *Staphylococcus aureus* Collagen Adhesin Contributes to the Pathogenesis of Osteomyelitis. *Bone* **2002**, *30*, 275−280.

(8) Rhem, M. N.; Lech, E. M.; Patti, J. M.; McDevitt, D.; Höök, M.; Jones, D. B.; Wilhelmus, K. R. The Collagen-Binding Adhesin is a Virulence Factor in *Staphylococcus aureus* Keratitis. *Infect. Immun.* **2000**, *68*, 3776−3779.

(9) Kang, M.; Ko, Y. P.; Liang, X.; Ross, C. L.; Liu, Q.; Murray, B. E.; Höök, M. Collagen-Binding Microbial Surface Components Recognizing Adhesive Matrix Molecule (MSCRAMM) of Gram-Positive Bacteria Inhibit Complement Activation *via* the Classical Pathway. *J. Biol. Chem.* **2013**, *288*, 20520−20531.

(10) Lopes, J.; Dos Reis, M.; Brentani, R. Presence of Laminin Receptors in *Staphylococcus aureus*. *Science* **1985**, *229*, 275−277.

(11) Shinji, H.; Seki, K.; Tajima, A.; Uchida, A.; Masuda, S. Fibronectin Bound to the Surface of *Staphylococcus aureus* Induces Association of Very Late Antigen 5 and Intracellular Signaling Factors with Macrophage Cytoskeleton. *Infect. Immun.* **2003**, *71*, 140−146.

(12) Liu, Q.; Ponnuraj, K.; Xu, Y.; Ganesh, V. K.; Sillanpää, J.; Murray, B. E.; Höök, M. The *Enterococcus faecalis* MSCRAMM ACE Binds Its Ligand by the Collagen Hug Model. *J. Biol. Chem.* **2007**, *282*, 19629−19637.

(13) Nallapareddy, S. R.; Qin, X.; Weinstock, G. M.; Höök, M.; Murray, B. E. *Enterococcus faecalis* Adhesin, Ace, Mediates Attachment to Extracellular Matrix Proteins Collagen Type IV and Laminin as well as Collagen Type I. *Infect. Immun.* **2000**, *68*, 5218−5224.

(14) Switalski, L.; Speziale, P.; Höök, M. Isolation and Characterization of a Putative Collagen Receptor from *Staphylococcus aureus* Strain Cowan 1. *J. Biol. Chem.* **1989**, *264*, 21080−21086.

(15) Switalski, L. M.; Patti, J. M.; Butcher, W.; Gristina, A. G.; Speziale, P.; Höök, M. A Collagen Receptor on *Staphylococcus aureus* Strains Isolated from Patients with Septic Arthritis Mediates Adhesion to Cartilage. *Mol. Microbiol.* **1993**, *7*, 99−107.

(16) Xiao, J.; Dufrêne, Y. F. Optical and Force Nanoscopy in Microbiology. *Nat. Microbiol.* **2016**, *1*, 16186.

(17) Alsteens, D.; Pfreundschuh, M.; Zhang, C.; Spoerri, P. M.; Coughlin, S. R.; Kobilka, B. K.; Müller, D. J. Imaging G Protein-Coupled Receptors while Quantifying Their Ligand-Binding Free-Energy Landscape. *Nat. Methods* **2015**, *12*, 845−851.

(18) Becherelli, M.; Prachi, P.; Viciani, E.; Biagini, M.; Fiaschi, L.; Chiarot, E.; Fontana, M. R.; et al. Protective Activity of the CnaBE3 Domain Conserved Among *Staphylococcus aureus* Sdr Proteins. *PLoS One* **2013**, *8*, e74718.

(19) Visai, L.; Xu, Y.; Casolini, F.; Rindi, S.; Höök, M.; Speziale, P. Monoclonal antibodies to CNA, a Collagen-binding Microbial Surface Component Recognizing Adhesive Matrix Molecules, Detach *Staphylococcus aureus* from a Collagen Substrate. *J. Biol. Chem.* **2000**, *275*, 39837−39845.

(20) Schulze-Koops, H.; Burkhardt, H.; Heesemann, J.; Von Der Mark, K.; Emmrich, F. Plasmid-Encoded Outer Membrane Protein YadA Mediates Specific Binding of Enteropathogenic yersiniae to Various Types of Collagen. *Infect. Immun.* **1992**, *60*, 2153−2159.

(21) Flügel, A.; Schulze-Koops, H.; Heesemann, J.; Kühn, K.; Sorokin, L.; Burkhardt, H.; Emmrich, F. Interaction of Enteropathogenic *Yersinia enterocolitica* with Complex Basement Membranes and the Extracellular Matrix Proteins Collagen Type IV, Laminin-1 and-2, and Nidogen/Entactin. *J. Biol. Chem.* **1994**, *269*, 29732−29738.

(22) Skurnik, M.; El Tahir, Y.; Saarinen, M.; Jalkanen, S.; Toivanen, P. YadA Mediates Specific Binding of Enteropathogenic *Yersinia enterocolitica* to Human Intestinal Submucosa. *Infect. Immun.* **1994**, *62*, 1252−1261.

(23) Somarajan, S. R.; La Rosa, S. L.; Singh, K. V.; Roh, J. H.; Höök, M.; Murray, B. E. The Fibronectin-Binding Protein fnm Contributes to Adherence to Extracellular Matrix Components and Virulence of *Enterococcus faecium*. *Infect. Immun.* **2015**, *83*, 4653−4661.

(24) Rich, R. L.; Kreikemeyer, B.; Owens, R. T.; LaBrenz, S.; Narayana, S. V.; Weinstock, G. M.; Höök, M. Ace is a Collagen-Binding MSCRAMM from *Enterococcus faecalis*. *J. Biol. Chem.* **1999**, *274*, 26939−26945.

(25) Pfaff, M.; Göhring, W.; Brown, J. C.; Timpl, R. Binding of Purified Collagen Receptors ($\alpha1\beta1$, $\alpha2\beta1$) and RGD-Dependent Integrins to Laminins and Laminin Fragments. *Eur. J. Biochem.* **1994**, *225*, 975−984.

(26) Sung, U.; O'Rear, J. J.; Yurchenco, P. D. Cell and Heparin Binding in the Distal Long Arm of Laminin: Identification of Active and Cryptic Sites with Recombinant and Hybrid Glycoprotein. *J. Cell Biol.* **1993**, *123*, 1255−1268.

(27) Rich, R. L.; Deivanayagam, C. C.; Owens, R. T.; Carson, M.; Höök, A.; Moore, D.; Yang, V. W.-C.; Narayana, S. V. L.; Höök, M. Trench-Shaped Binding Sites Promote Multiple Classes of Interactions Between Collagen and the Adherence Receptors, $\alpha1\beta1$ Integrin and *Staphylococcus aureus* Cna MSCRAMM. *J. Biol. Chem.* **1999**, *274*, 24906−24913.

(28) Hartford, O.; Francois, P.; Vaudaux, P.; Foster, T. The Dipeptide Repeat Region of the Fibrinogen-Binding Protein (Clumping Factor) is Required for Functional Expression of the Fibrinogen-Binding Domain on the *Staphylococcus aureus* Cell Surface. *Mol. Microbiol.* **1997**, *25*, 1065−1076.

(29) Ebner, A.; Wildling, L.; Kamruzzahan, A. S. M.; Rankl, C.; Wruss, J.; Hahn, C. D.; et al. A New, Simple Method for Linking of

DOI: 10.1021/acsnano.6b08404
ACS Nano 2017, 11, 2160−2170

Antibodies to Atomic Force Microscopy Tips. *Bioconjugate Chem.* **2007**, *18*, 1176−1184.
(30) Beaussart, A.; El-Kirat-Chatel, S.; Sullan, R. M. A.; Alsteens, D.; Herman, P.; Derclaye, S.; Dufrêne, Y. F. Quantifying the Forces Guiding Microbial Cell Adhesion Using Single-Cell Force Spectroscopy. *Nat. Protoc.* **2014**, *9*, 1049−1055.
(31) Beaussart, A.; El-Kirat-Chatel, S.; Herman, P.; Alsteens, D.; Mahillon, J.; Hols, P.; Dufrêne, Y. F. Single-Cell Force Spectroscopy of Probiotic Bacteria. *Biophys. J.* **2013**, *104*, 1886−1892.

DOI: 10.1021/acsnano.6b08404
ACS Nano 2017, 11, 2160−2170